Polymer 54 (2013) 1691–1699

Contents lists available at SciVerse ScienceDirect

Polymer

journal homepage: www.elsevier.com/locate/polymer

Further studies on Mori–Tanaka models for thermal expansion coefficients of composites

Pin Lu

*Institute of Materials Research and Engineering, A*STAR (Agency for Science, Technology and Research), 3 Research Link, Singapore 117602, Singapore*

ARTICLE INFO

Article history:
Received 23 July 2012
Accepted 14 January 2013
Available online 25 January 2013

Keywords:
Composites
Thermal expansion
Mori–Tanaka model

ABSTRACT

The relations of Mori–Tanaka (M–T) model for thermal expansion coefficients (CTEs) of composites are derived following a regular procedure to compare with other two different expressions of M–T model often used for modeling thermal properties of nanocomposites. It is verified that by correcting the related parameters mis-determined all the relations are consistent and can provide same predicting results. This clarifies the confused information in literature concerning the M–T model on CTEs. Some issues are discussed and attentions are suggested in appropriate use of different relations of M–T models. Comparisons of M–T model with other related theory models on CTEs are made by numerical results, which show some advantages of M–T relations over other models in applications. The related expressions of M–T model on CTEs are summed up under self-consistent coordinate systems for convenience of practical use.

1. Introduction

In a recent paper by Lee et al. [1], a model for predicting effective coefficients of thermal expansion (CTE) of composites was presented, and the predicted results were shown to be different from those calculated by the model of Chow [2,3]. It is noted that although derived in different manners, the models both in Ref. [1] and in Ref. [3] are established essentially by using the equivalent inclusion idea of Eshelby [4] and the mean-field approach of Mori–Tanaka (M–T) [5]. However, it has been verified by Benveniste and Dvorak [6] that the results derived following the concepts of Eshelby [4] and M–T [5], despite with different expressions, are basically equivalent. Owing to importance of M–T based models in predicting mechanical and thermal properties of composite materials, it is thus necessary to clarify the confusions raised by [1] and [6], which would be very useful in correct use of M–T models in engineering applications. This motivates the present work.

Analyses of thermoelastic properties of composite materials have drawn considerable interest in literature. Many micromechanics models and bound relations have been suggested to predict effective coefficients of thermal expansion of various composites. The earlier models by Turner [7] and Kerner [8] provide simple relations, which are often used as a lower and an upper bound, respectively, for predicting CTEs of composites. Levin [9] developed a model for determining composite CTE based on the effective elastic properties of the composites. Levin's work was extended by Schapery [10] and Rosen and Hashin [11] and refined bounds and relations on CTE were derived. In these models, the effective elastic properties of composites have to be known before estimating their effective thermal properties. This might be inconvenient since prediction relations based on mechanical and thermal properties of component materials only are more desirable in practical uses. Furthermore, filler aspect ratio and orientation effects cannot be well accounted in these models. Brief review and comparison of these bounds and relations can be found in [12,13]. On the other hand, the models in [1–3,14–21] for composite CTE analysis were derived by making use of the methods of Eshelby [4] and Mori–Tanaka [5]. These M–T models, other than Levin and R–H relations, account for effect of filler aspect ratio and are directly related to mechanical and thermal properties of matrix and fillers only. Therefore, the M–T models on CTE have received increasing attentions in recent years, especially for predicting CTEs on nanocomposites of plate-like (i.e. nano clay) or fiber-like (i.e. carbon nanotube) fillers [1,21–25] in which filler aspect ratio and orientation effects play important roles on overall material properties.

In the work by Benveniste and Dvorak [6], the effective thermal expansion coefficients of M–T method are derived based on the approaches of Benveniste [26] for the exposition of Mori–Tanaka theory, and are then proved to be consistent with other M–T results derived in different ways. Especially, by applying the approaches of Eshelby and Mori–Tanaka, Chow [3] and Lee et al. [1] have, respectively,

E-mail addresses: lup@imre.a-star.edu.sg, pinlu01@gmail.com.

0032-3861/$ – see front matter © 2013 Elsevier Ltd. All rights reserved.
http://dx.doi.org/10.1016/j.polymer.2013.01.021

obtained the explicit expressions of M–T models on CTEs incorporating the parameter of filler aspect ratio for aligned composites, which are often used for predicting thermal properties of nanocomposites [22–25]. According to the consistency demonstration made in [6], however, the relations by Chow [3] and by Lee et al. [1] must give same predicting results. The present work is to verify this.

To this end, the general relations of composites CTEs in the forms of tensor notations are derived first rigorously following the standard procedures on Eshelby and M–T approaches summarized by Mura [27]. The results are verified to be consistent with those by Benveniste and Dvorak [6]. The explicit expressions for aligned composites are then derived based on the general relations obtained, and are compared with the related expressions presented in [3] and [1] for verification. For completeness of the work, the general relations of CTEs for multi-phase composites with fillers of different materials, and the CTEs of composites with 3-dimensional (3D) and 2-dimensional (2D) randomly distributed fillers are also presented. Finally, calculated examples are given to compare M–T results with those predicted by other theory models, and some issues and attentions in proper applying different relations of M–T models for predictions are discussed.

2. Theory

Consider a composite with finite volume fractions of matrix and filler phases defined by ϕ_m and ϕ_f, respectively, which follow the relation $\phi_m+\phi_f=1$. The elastic moduli tensors in the phases are denoted by C^m and C^f respectively, and the thermal expansion coefficients of the matrix and the fillers are denoted by α^m and α^f, respectively. The super and subscripts m and f represent the matrix and the filler, respectively.

Assume the composite is subjected to a uniform temperature change ΔT, a misfit strain caused by the difference of the thermal expansion coefficients between the matrix and the filler is given by

$$\varepsilon^{\Delta T} = \left(\alpha^f - \alpha^m\right)\Delta T \tag{1}$$

With the uniform temperature change, the thermal expansion in the homogeneous matrix without any inclusion is uniform and the elastic field in the matrix is not generated. However, a certain average perturbed strain $\tilde{\varepsilon}^m$ has been introduced due to the presence of fillers. This perturbed strain corresponds to an average perturbed stress $\tilde{\sigma}^m$ through the elastic constants C^m of the matrix. Thus, the constitutive relation in the matrix after the perturbation is

$$\tilde{\sigma}^m = C^m\tilde{\varepsilon}^m \tag{2}$$

Furthermore, define $\tilde{\sigma}^f$ and $\tilde{\varepsilon}^f$ to be the average perturbed stress and strain in the filler with respect to the matrix. According to Eshelby equivalent principle [4], the average stress in the particle may be written as [27]

$$\tilde{\sigma}^m + \tilde{\sigma}^f = C^f\left(\tilde{\varepsilon}^m + \tilde{\varepsilon}^f - \varepsilon^{\Delta T}\right) = C^m\left(\tilde{\varepsilon}^m + \tilde{\varepsilon}^f - \varepsilon^{\Delta T} - \varepsilon^*\right) \tag{3}$$

where $\varepsilon^{\Delta T}$ is the misfit strain given in Eq. (1), ε^* is the average equivalent transformation strains of the particle and is a fictitious one. According to Eshelby solutions for the inhomogeneity with its own eigenstrains [27, pp. 179–81], we have

$$\tilde{\varepsilon}^f = S\varepsilon^{**} \tag{4}$$

where S is Eshelby tensors for the domain of the particle, and ε^{**} is the total eigenstrain on the inclusion:

$$\varepsilon^{**} = \varepsilon^{\Delta T} + \varepsilon^* \tag{5}$$

Since the composite is not subjected any external traction, the average of the stresses over the matrix and fillers should be zero, i.e. $\phi_m\tilde{\sigma}^m + \phi_f(\tilde{\sigma}^m + \tilde{\sigma}^f) = 0$ or $\tilde{\sigma}^m + \phi_f\tilde{\sigma}^f = 0$. From Eqs. (2) and (3), and making use of the relations in Eqs. (4) and (5), this gives

$$\tilde{\varepsilon}^m = -\phi_f\left(\tilde{\varepsilon}^f - \varepsilon^{\Delta T} - \varepsilon^*\right) = -\phi_f(S-I)\varepsilon^{**} \tag{6}$$

substituting Eqs. (4)–(6) into Eq. (3) yields

$$\left\{\left(C^f - C^m\right)\left[S - \phi_f(S-I)\right] + C^m\right\}\varepsilon^{**} = C^f\varepsilon^{\Delta T} \tag{7}$$

from which the total eigenstrain ε^{**} can be solved in term of $\varepsilon^{\Delta T}$ as

$$\varepsilon^{**} = \left\{\left(C^f - C^m\right)\left[S - \phi_f(S-I)\right] + C^m\right\}^{-1}C^f\varepsilon^{\Delta T} \tag{8}$$

On the other hand, the volume average strain of the composite caused by $\varepsilon^{\Delta T}$ is given by $\overline{\varepsilon} = \phi_m\tilde{\varepsilon}^m + \phi_f(\tilde{\varepsilon}^m + \tilde{\varepsilon}^f)$. From Eqs. (4) and (6), this gives [27, pp. 388–90].

$$\overline{\varepsilon} = \phi_f\varepsilon^{**} \tag{9}$$

The total average strain over the whole composite under the uniform temperature change is the sum of the thermal strain of matrix, $\alpha^m\Delta T$, generated by the temperature change and the average strain $\overline{\varepsilon}$ due to the total eigenstrain in the equivalent particles, i.e.,$\overline{\varepsilon}^{\text{total}} = \alpha^m\Delta T + \overline{\varepsilon}$. According to the definition of thermal expansion coefficient, the total average strain in the composite by ΔT can be expressed as $\overline{\varepsilon}^{\text{total}} = \overline{\alpha}\Delta T$. The effective thermal expansion coefficient of the composite, $\overline{\alpha}$, thus is given by

$$\overline{\alpha} = \alpha^m + \phi_f\varepsilon^{**}/\Delta T \tag{10}$$

By substituting Eqs. (8) and (1) into Eq. (10), we obtain the effective thermal expansion coefficient as

$$\overline{\alpha} = \alpha^m + \phi_f\left\{\left(C^f - C^m\right)\left[S - \phi_f(S-I)\right] + C^m\right\}^{-1}C^f\left(\alpha^f - \alpha^m\right) \tag{11}$$

The details of the derivations presented above can be found in Mura [27], and are similar as those given in Refs. [17,20]. It has been verified [6] that the effective thermal expansion coefficient given in Eq. (11) is consistent with that obtained by Benveniste and Dvorak [6] derived in a different way. By comparing with the derivations in Ref. [6], the present approaches seem to be more straightforward and the results expressed in the form of Eq. (11) are relatively compact and concise.

The solutions in Eq. (11) are for two phase composites consisting of fillers of same materials. The results can be extended to multiphase composites with N types of inclusions of different materials,

$$\begin{aligned}\overline{\alpha} = \alpha^m + \sum_{i=1}^{N}\phi_{f_i}\left\{\left(C^{f_i} - C^m\right)\left[S^{f_i} - \sum_{i=1}^{N}\phi_{f_i}\left(S^{f_i} - I\right)\right] + C^m\right\}^{-1} \\ \times C^{f_i}\left(\alpha^{f_i} - \alpha^m\right)\end{aligned} \tag{12}$$

where C^{f_i} is the elastic moduli tensor, α^{f_i} is the thermal expansion coefficient tensor, S^{f_i} is the Eshelby tensor and ϕ_{fi} is the volume fraction of the ith filler phase ($i = 1,2,\ldots,N$), respectively. The related derivations can be referred to Appendix 1.

3. Explicit expressions of M–T model

In this section, the explicit expressions of the general results Eq. (11) for composites with isotropic matrix and filler material properties are presented for the cases of aligned, 3D and 2D randomly distributed fillers, respectively. The explicit relations are especially useful in engineering applications.

3.1. Composites with unidirectionally aligned fillers

For spheroidal fillers ($a_1 \neq a_2 \neq a_3$) with x_1 to be the axis of rotation symmetry as shown in Fig. 1, the components of Eshelby tensor $\boldsymbol{S}$ are given in Appendix 2. It is assumed that the spheroidal inclusions (fillers) are aligned along the $x_1$direction in matrix. Since both the matrix and filler phases are taken to be isotropic, the components of $\boldsymbol{C}^m$ for the matrix phase and $\boldsymbol{C}^f$ for the filler phase and the misfit strain can be written as

$$C^{\chi}_{ijkl} = \lambda_\chi \delta_{ij}\delta_{kl} + \mu_\chi\left(\delta_{ik}\delta_{jl} + \delta_{il}\delta_{jk}\right),\ (\chi = m,f),\ \varepsilon^{\Delta T}_{ij} = \left(\alpha_f - \alpha_m\right)\Delta T \delta_{ij} \tag{13}$$

where λ_χ and μ_χ ($\chi = m,f$) are the Lame constants, defined by $\lambda = Ev/[(1+v)(1-2v)]$ and $\mu = E/[2(1+v)]$, α_m and α_f are the isotropic thermal expansion coefficients of the matrix and fillers, respectively, and δ_{ij} is the Kronecker delta. With the materials constants, Eq. (7) can be written in the form of matrix components as

$$\left(C^f_{ijkl} - C^m_{ijkl}\right)\left[\left(1-\phi_f\right)S_{klmn}\varepsilon^{**}_{mn} + \phi_f \varepsilon^{**}_{kl}\right] + C^m_{ijkl}\varepsilon^{**}_{kl} = C^f_{ijkl}\varepsilon^{\Delta T}_{kl} \tag{14}$$

from which the nonzero components ε^{**}_{ii} ($i = 1,2,3$) can be solved from the linear equations

$$\begin{aligned}
B_1\varepsilon^{**}_{11} + B_2\varepsilon^{**}_{22} + B_2\varepsilon^{**}_{33} &= D_0\left(\alpha_f - \alpha_m\right)\Delta T \\
B_3\varepsilon^{**}_{11} + B_4\varepsilon^{**}_{22} + B_5\varepsilon^{**}_{33} &= D_0\left(\alpha_f - \alpha_m\right)\Delta T \\
B_3\varepsilon^{**}_{11} + B_5\varepsilon^{**}_{22} + B_4\varepsilon^{**}_{33} &= D_0\left(\alpha_f - \alpha_m\right)\Delta T
\end{aligned} \tag{15}$$

where the parameters B_i are [28,1]

$$\begin{aligned}
B_1 &= \phi_f D_1 + D_2 + \left(1-\phi_f\right)(D_1 S_{1111} + 2S_{2211}) \\
B_2 &= \phi_f + D_3 + \left(1-\phi_f\right)(D_1 S_{1122} + S_{2222} + S_{2233}) \\
B_3 &= \phi_f + D_3 + \left(1-\phi_f\right)[S_{1111} + (1+D_1)S_{2211}] \\
B_4 &= \phi_f D_1 + D_2 + \left(1-\phi_f\right)(S_{1122} + D_1 S_{2222} + S_{2233}) \\
B_5 &= \phi_f + D_3 + \left(1-\phi_f\right)(S_{1122} + S_{2222} + D_1 S_{2233})
\end{aligned} \tag{16}$$

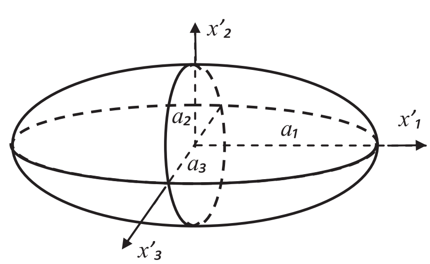

Fig. 1. Coordinate system used in this paper for describing ellipsoidal inclusion (aspect ratio $a = a_1/a_3$).

and

$$\begin{aligned}
&D_1 = 1 + 2\left(\mu_f - \mu_m\right)/\left(\lambda_f - \lambda_m\right),\ D_2 = (\lambda_m + 2\mu_m)/\left(\lambda_f - \lambda_m\right) \\
&D_3 = \lambda_m/\left(\lambda_f - \lambda_m\right),\ D_0 = \left(3\lambda_f + 2\mu_f\right)/\left(\lambda_f - \lambda_m\right)
\end{aligned} \tag{17}$$

By solving the linear equations Eq. (15), we obtain

$$\begin{aligned}
\varepsilon^{**}_{11} &= \frac{(2B_2 - B_4 - B_5)D_0}{2B_2B_3 - B_1(B_4 + B_5)}\left(\alpha_f - \alpha_m\right)\Delta T \\
\varepsilon^{**}_{22} = \varepsilon^{**}_{33} &= \frac{(B_3 - B_1)D_0}{2B_2B_3 - B_1(B_4 + B_5)}\left(\alpha_f - \alpha_m\right)\Delta T
\end{aligned} \tag{18}$$

and from Eq. (14), we have $\varepsilon^{**}_{ij} = 0$ ($i \neq j$). By substituting the values of ε^{**}_{ij} into Eq. (10), the components of the effective thermal expansion coefficients are obtained as

$$\begin{aligned}
\alpha_{11} &= \alpha_m + \phi_f \frac{(2B_2 - B_4 - B_5)D_0}{2B_2B_3 - B_1(B_4 + B_5)}\left(\alpha_f - \alpha_m\right) \\
\alpha_{22} = \alpha_{33} &= \alpha_m + \phi_f \frac{(B_3 - B_1)D_0}{2B_2B_3 - B_1(B_4 + B_5)}\left(\alpha_f - \alpha_m\right)
\end{aligned} \tag{19}$$

It is seen that for the spheroidal fillers, the mechanical and thermal properties of the aligned filler composites are isotropic in transversal plane.

By comparing the above relations with similar ones given in Eqs. (21) and (22) of [1], it is found that the parameter D_4 defined in those relations was mis-determined, which should be corrected by $(\alpha_f - \alpha_m)D_0$.

3.2. Composites with randomly distributed fillers

After the effective thermal expansion coefficients of the composites with aligned fillers are obtained, the effective thermal expansion coefficients of composites with randomly oriented fillers can be calculated by orientation average for the second-order effective thermal expansion coefficient tensor of the aligned fillers, α_{ii}, over 3D or 2D spaces as shown in Refs. [16,19]. The results are given below.

For 3D randomly distributed fillers, the effective mechanical and thermal properties of the composites are isotropic. Therefore, there is only one independent effective thermal expansion coefficient, which gives

$$\langle\overline{\alpha}\rangle_{3D} = \frac{1}{3}\alpha_{11} + \frac{2}{3}\alpha_{22} \tag{20}$$

For 2D randomly distributed fillers, the effective mechanical and thermal properties of the composites are transversely isotropic. Since $a_2 = a_3$ for spheroidal inclusions, by taking local axis x'_2 or x'_3 (as shown in Fig. 1) perpendicular to the x_2x_3 plane of the global coordinate system, and the spheroidal fillers are randomly oriented in the x_2x_3 plane, which is the transversely isotropic plane. In this case, the components of the effective thermal expansion coefficients under the global coordinate system are given by

$$\langle\overline{\alpha}_{11}\rangle_{2D} = \alpha_{22},\quad \langle\overline{\alpha}_{22}\rangle_{2D} = \langle\overline{\alpha}_{33}\rangle_{2D} = \frac{1}{2}(\alpha_{11} + \alpha_{22}) \tag{21}$$

3.3. Review of Chow relations [3]

In different models on CTEs of composites available in literature, the relations obtained by Chow [3] are capable of investigating influence of filler aspect ratio effects, and have been considerably used for predicting thermal properties of polymer composites [22–25]. In using Chow's relations, it should be noted that the spheroidal inclusion in Refs. [2,3] is defined by the equation

$(x_1^2+x_2^2)/a_1^2+x_3^2/a_3^2 = 1$, i.e. x_3 being the axis of rotation symmetry, and the aspect ratio ρ in Refs. [2,3] is defined by $\rho = a_3/a_1$. These are different from the definitions of the coordinate system for spheroidal inclusion shown in Fig. 1, which are commonly used in present literature. Since the components of Eshelby tensor are directly related to the coordinate system defined for the spheroidal inclusion, the components with same subscript numbers under different coordinate systems may have different expressions. Therefore, when using Chow's relations under the coordinate system for spheroidal inclusion shown in Fig. 1, it should be realized that the subscript numbers of the Eshelby tensor components in related coefficients of Chow's original expressions must be permuted accordingly. This has been overlooked in some applications, which may lead to incorrect prediction results.

For convenience of future applications, the relations for predicting CTE in Chow model [2,3] for a spheroidal inclusion defined with the symmetric axis identified as x_1, as shown in Fig. 1, are given below

$$\begin{aligned} \alpha_{11} &= \alpha_m + \phi_f \frac{\tilde{G}_1}{2\tilde{K}_1\tilde{G}_3+\tilde{G}_1\tilde{K}_3}\frac{K_f}{K_m}\left(\gamma_f-\gamma_m\right) \\ \alpha_{22} &= \alpha_{33} = \alpha_m + \phi_f \frac{\tilde{G}_3}{2\tilde{K}_1\tilde{G}_3+\tilde{G}_1\tilde{K}_3}\frac{K_f}{K_m}\left(\gamma_f-\gamma_m\right) \end{aligned} \tag{22}$$

where $\gamma_m = 3\alpha_m$ and $\gamma_f = 3\alpha_f$ are the bulk CTEs of the matrix and filler ($\gamma = \alpha_{11}+\alpha_{22}+\alpha_{33}$), respectively, K_m and K_f are the bulk moduli of the matrix and fillers, respectively, given by $K = E/[3(1-2v)']$, and the coefficients $\tilde{K}_i$and $\tilde{G}_i$ are given by

$$\begin{aligned} \tilde{K}_i &= 1+\left(K_f/K_m-1\right)\left[\left(1-\phi_f\right)b_i+\phi_f\right] \\ \tilde{G}_i &= 1+\left(G_f/G_m-1\right)\left[\left(1-\phi_f\right)c_i+\phi_f\right] \end{aligned} \tag{23}$$

and

$$\begin{aligned} b_1 &= S_{2222}+S_{3322}+S_{1122}, \quad & b_3 &= S_{2211}+S_{3311}+S_{1111} \\ c_1 &= S_{2222}+S_{2233}-2S_{1122} \quad & c_3 &= S_{1111}-S_{2211} \end{aligned} \tag{24}$$

where S_{ijkl} are the components of Eshelby tensor consistent with the coordinate system for spheroidal inclusion shown in Fig. 1, which are given in Appendix 2. For spherical inclusions with $a_1 = a_2 = a_3$, b_i and c_i in Eq. (24) reduce to

$$b_1 = b_3 = \frac{1+v_m}{3(1-v_m)}, \quad c_1 = c_3 = \frac{2(4-5v_m)}{15(1-v_m)} \tag{25}$$

It is noted that the coefficients b_i and c_i in Eq. (24) are apparently different from the corresponding ones α_i and β_i given in page 962 of [2], but they are identical under the respective coordinate systems defined, i.e. $b_i = \alpha_i$ and $c_i = \beta_i$.

By substituting the components S_{ijkl} given in Appendix 2 into Eq. (24), the explicit expressions of b_i and c_i can be obtained, which can be found in the Appendix of [2] or the electronic supplementary information for [24]. However, it should be pointed out that the parameter α_3 given in the Appendix of [2] is incorrect, which should be read as $\alpha_3 = 4\pi Q/3 - 4(I-\pi)R$.

It can be verified that the relations given in Eqs. (24) and (19) can provide same predicting results. This indicates that the relations given in Eq. (24) are actually identical to those given in Eq. (19). They are just different expressions of M–T model. Therefore, for *spheroidal* inclusion model, one can select either one for predictions in practical applications.

3.4. General relations of M–T model

It is known that the relations given in Eqs. (19) and (24) are limited to the case for spheroidal inclusion ($a_1 \neq a_2 \equiv a_3$) with x_1 to be the axis of rotation symmetry. For general situations of composites with ellipsoidal inclusions ($a_1 \neq a_2 \neq a_3$), Eqs. (19) and (24) are not available. To calculate the problems, one can still start from the linear equations in Eq. (14). However, the components S_{klmn} of Eshelby tensor now are not those given in Appendix 2 for the spheroidal inclusions. The expressions of Eshelby tensor for ellipsoidal inclusions can be found in Chapter 2 of [27]. By substituting the related components for the ellipsoidal inclusions into Eq. (14), the components ε_{ii}^{**} of the total eigenstrain on the inclusions can be readily obtained by solving the linear equations. The CTEs for composites with ellipsoidal fillers can then be predicted by Eq. (10). Since there is no any axis of rotation symmetry for ellipsoidal inclusion, the mechanical and thermal properties of the aligned filler composites are orthotropic in transversal plane, i.e. $\alpha_{22} \neq \alpha_{33}$. A related work has been reported in Ref. [21]. However, it seemed there was an error in Eq. (4) of [21].

4. Comparison and discussion

In this section, the results of M–T model on CTE presented above are compared with several other theory models often used in literature. Some related properties and applicable ranges of different models are discussed based on the material data of given example.

4.1. Relations of several theory models on CTEs

In the theory models other than M–T models on CTE available in literature, the relations of rule of mixture (ROM) model, Turner model [7], Kerner model [8] and Schapery simplified model [10] can provide direct predictions using mechanical and thermal properties of component materials only. There are also some other popular models, such as Levin [9], Schapery [10] and Rosen and Hashin [11] models, which require known effective elastic properties of composites before estimating their effective thermal properties as reviewed in introduction. For convenience, ROM, Turner, Kerner and Schapery models are taken for comparison in this work. Their relations are given below:

- *Rule of mixture (ROM) model*

$$\alpha = \alpha_m\phi_m + \alpha_f\phi_f \tag{26}$$

where α is effective coefficient of thermal expansion (CTE) of composites.

- *Turner model* [7]

$$\alpha = \left(\alpha_m\phi_m K_m + \alpha_f\phi_f K_f\right)\Big/\left(\phi_m K_m + \phi_f K_f\right) \tag{27}$$

- *Kerner model* [8]

$$\alpha = \alpha_m\phi_m + \alpha_f\phi_f + \left(\alpha_f - \alpha_m\right)\phi_m\phi_f\frac{K_f - K_m}{\phi_m K_m + \phi_f K_f + 3K_m K_f/4G_m} \tag{28}$$

where $G_m$is the shear modulus of the matrix, given by $G = E/[2(1+v)]$.

Table 1
Material properties of epoxy resin and glass fibers.

	Density (kg/m^3)	Modulus (GPa)	Linear CTE $\times 10^6$ (K^{-1})	Poisson ratio
Epoxy	1200	E_m 2.76	α_m 81	ν_m 0.35
Glass fiber	2540	E_f 72.4	α_f 5.0	ν_f 0.20

- *Schapery model* [10]

For unidirectional fiber reinforce composites and assuming that the Poisson ratios of the matrix and fiber are equal, the approximate relations of Schapery model on CTEs in axial and transversal directions, respectively, are given below

$$\begin{aligned}\alpha_{11} &= \left(\alpha_m\phi_m E_m + \alpha_f\phi_f E_f\right)\Big/\left(\phi_m E_m + \phi_f E_f\right)\\ \alpha_{22} &= (1+\nu_m)\alpha_m\phi_m + \left(1+\nu_f\right)\alpha_f\phi_f - \alpha_{11}\left(\nu_m\phi_m + \nu_f\phi_f\right)\end{aligned} \tag{29}$$

It is noted that all of the relations in Eqs. (26)–(29) do not include the parameter of filler aspect ratio. They are not suitable for predictions of composites with fillers' geometry shape effects.

4.2. Numerical results and discussion

In the numerical calculations, the material properties of the epoxy resin matrix and the glass fillers taken from Ref. [1] are used, which are listed in Table 1.

Fig. 2 shows the changes of normalized CTEs with fillers' volume fraction ϕ_f for the fiber-like fillers with the aspect ratio $a = 10$ calculated by the relations Eq. (19) or Eq. (22) of the aligned M–T model, which are compared with Turner and Schapery predictions. Since the linear CTE of the fillers is smaller than that of the matrix as shown in Table 1, it is seen that the effective longitudinal CTEs α_{11} along the fiber alignment direction predicted by all models decrease monotonically with the increase of ϕ_f and reach to the fillers' CTE at $\phi_f = 1$, meaning that α_{11} is always smaller than α_m of the matrix for the aligned fiber-like composites. However, it is interesting to see that the normalized effective CTEs α_{22}/α_m or α_{33}/α_m in the transversal direction predicted by both M–T and Schapery models increase at the initial stages and then decrease with the increase of ϕ_f, meaning that in certain regions of small fillers' volume fractions ($0 < \phi_f < 0.15$ for M–T and $0 < \phi_f < 0.25$ for Schapery models) the effective transversal CTE α_{22} or α_{33} is greater than α_m of the matrix for the composites. The thermal expansion properties for this kind of aligned fiber-like polymer composites are especially important because fillers' volume fractions for polymer composites are commonly in this range. Furthermore, it is also observed that for the aligned *fiber-like* polymer composites the effective transversal CTE α_{22} or α_{33} is greater than the longitudinal one, α_{11}, along the fiber alignment direction. In addition, the prediction results by Turner model is plotted for comparison. It is seen that the Turner results are close to α_{22} of M–T model for the aspect ratio $a = 10$. Since both Turner and Schapery models do not rely on filler aspect ratio, the Turner results can only given approximate predictions of α_{11} for the composites with other fillers' aspect ratios, and Schapery's predictions provide upper bound for α_{22} or α_{33} and lower bound for α_{11} of the fiber-like composites which can be seen more clearly from Fig. 4.

For comparison, the changes of normalized CTEs with fillers' volume fraction ϕ_f for the *disc-like* fillers with two cases of the aspect ratio $a < 1$ are plotted in Fig. 3 by the relations Eq. (19) or Eq. (22) of the aligned M–T model. It is seen that the positions of α_{11}/α_m and α_{33}/α_m in Figs. 2 and 3 are just reversed, i.e. α_{11} is greater than α_{33} in all ranges of the fillers' volume fractions for the aligned disc-like filler composites. Therefore, it is seen that Turner results are approximate predictions of α_{33} for $a = 0.01$ now. It is also shown in Fig. 3 that α_{11}/α_m increases and α_{33}/α_m decreases with the decrease of the aspect ratio a. To have an overall picture of how CTEs change with the aspect ratio, the predicted CTEs by M–T model for $10^{-3} < a < 10^3$ are shown in Fig. 4. It is seen that α_{11}/α_m decrease and α_{33}/α_m increase monotonically as the aspect ratio a increases from disc-like to fiber-like fillers, and $\alpha_{11} = \alpha_{22} = \alpha_{33}$ (isotropic property) at $a = 1$ which is the situation of spherical fillers. In addition, both α_{11}/α_m and α_{33}/α_m decrease with the increase of the fillers' volume fraction ϕ_f since $\alpha_f < \alpha_m$ as given in Table 1. Again, Fig. 4 shows that Schapery's results serve as upper bound of α_{33} and lower bound of α_{11} of M–T model for fiber-like aligned filler composites when $a \to \infty$. Therefore, Schapery relations given in Eq. (29) seem not suitable for composites with aligned disc-like fillers.

To investigate the influences of fillers' orientation effects on effective CTEs of composites, the variations of the effective CTEs with the aspect ratio a based on fillers' 2D random distribution as described by the relations Eq. (21) are shown in Fig. 5. It is seen that for the composites with this kind of fillers' 2D random distribution, $\langle\overline{\alpha}_{11}\rangle_{2D}/\alpha_m$ increase and $\langle\overline{\alpha}_{33}\rangle_{2D}/\alpha_m$ decrease monotonically as the

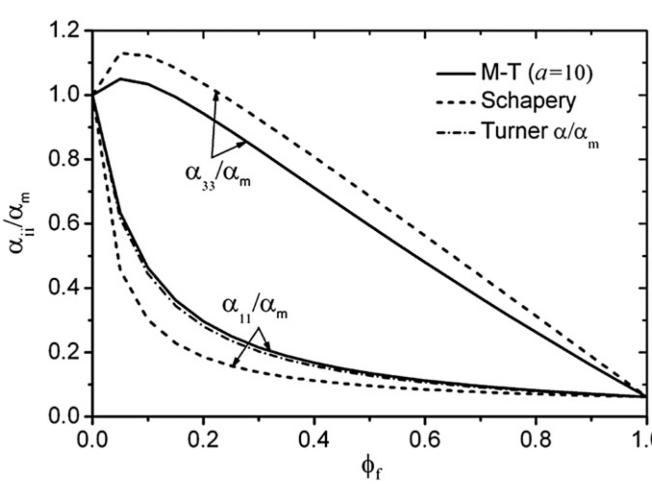

Fig. 2. Comparison of coefficients of thermal expansion by aligned M–T ($a = 10$), Schapery and Turner results.

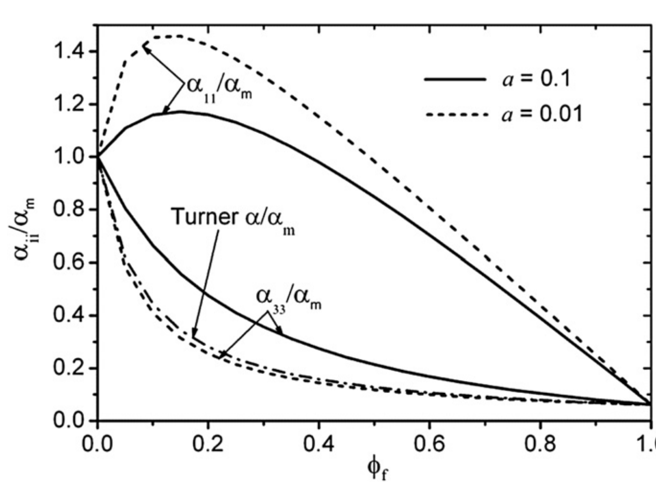

Fig. 3. Coefficients of thermal expansion by aligned M–T for aspect ratio $a < 1$ (disc-like inclusions).

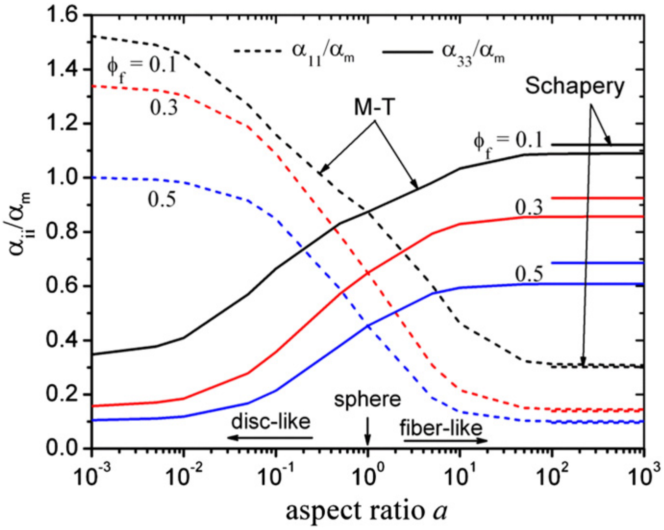

Fig. 4. Variation of coefficients of thermal expansion with aspect ratio a by aligned M–T and Schapery results.

aspect ratio a increases from disc-like to fiber-like fillers predicted by the M–T model, and $\langle\overline{\alpha}_{11}\rangle_{2D} < \langle\overline{\alpha}_{33}\rangle_{2D}$ for $a < 1$, $\langle\overline{\alpha}_{11}\rangle_{2D} > \langle\overline{\alpha}_{33}\rangle_{2D}$ for $a > 1$ and $\langle\overline{\alpha}_{11}\rangle_{2D} = \langle\overline{\alpha}_{33}\rangle_{2D}$ for the spherical fillers at $a = 1$. It is noted that for the composites with this kind of 2D random fillers, Schapery's predictions calculated by Eqs. (29) and (21) are upper bounds of both $\langle\overline{\alpha}_{11}\rangle_{2D}$ and $\langle\overline{\alpha}_{33}\rangle_{2D}$ of M–T results for composites with fiber-like fillers ($a > 1$).

For the composites with 3D randomly distributed fillers, the effective mechanical and thermal properties of the composites are isotropic. Fig. 6 shows the changes of the normalized CTE, $\langle\overline{\alpha}\rangle_{3D}/\alpha_m$, with fillers' volume fraction ϕ_f for the aspect ratios $a = 0.1$, 1 and 10, respectively, calculated by Eq. (19) (or Eq. (22)) together with Eq. (20) of the 3D random M–T model, which are compared with ROM, Turner, Kerner and Schapery predictions. It is seen that the results by Kerner and by M–T at $a = 1$ are same. It is not surprising because it has been verified that Kerner relation given in Eq. (28) is exactly that of M–T model for the spherical fillers at $a = 1$ [14,2]. It is also noted that the predicted results by Turner are significantly different

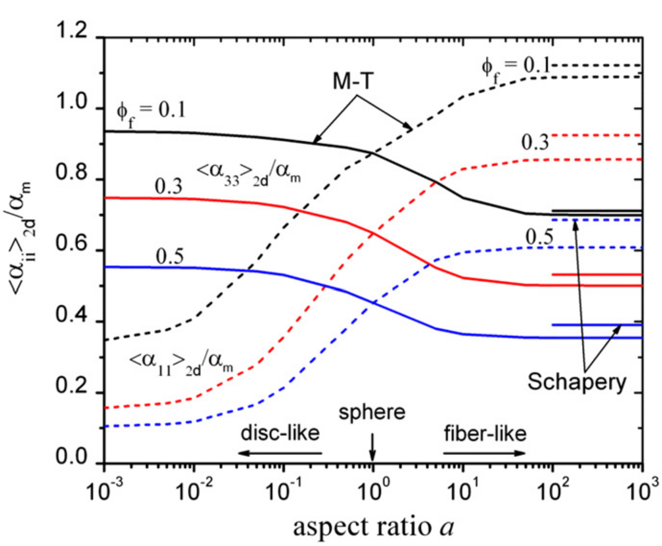

Fig. 5. Variation of coefficients of thermal expansion with aspect ratio a by 2D random M–T and Schapery results.

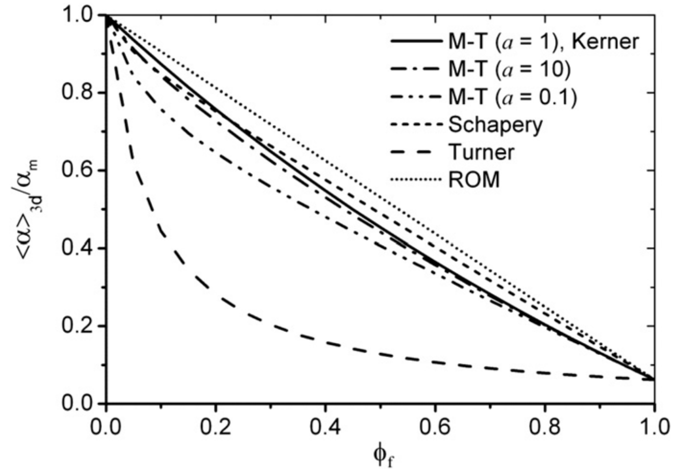

Fig. 6. Comparison of coefficients of thermal expansion by 3D ramdom M–T, ROM, Kerner, Schapery and Turner results.

from those by other models. Therefore, Turner model is not suitable for predicting CTE of composites with 3D randomly distributed fillers, and may be used for approximate predictions for composites with aligned fillers as shown in Figs. 2 and 3. Since Schapery model is related to M–T model for long fiber-like composites, it is seen that Schapery's results give relatively poor predictions for disc-like fillers with $a < 1$. The results by simple ROM model decrease linearly with ϕ_f, and can be applied as a crude upper bound of $\langle\overline{\alpha}\rangle_{3D}$. In Fig. 7, the variations of the effective CTEs with the aspect ratio a for the composites of 3D randomly distributed fillers are plotted. It is seen that $\langle\overline{\alpha}\rangle_{3D}/\alpha_m$ has the maximum value at $a = 1$ for spherical fillers, and decreases as a both increases in the fiber-like region and decreases in the disc-like regions. Therefore, Kerner's (or M–T at $a = 1$) prediction results can serve as upper bound of $\langle\overline{\alpha}\rangle_{3D}$ for M–T predictions of composites with 3D randomly distributed fillers. By comparing Fig. 7 with Figs. 4 and 5, it is seen that owing to 3D random distributions for fillers the predicted results for CTEs of 3D random model are not as sensitive to the fillers' aspect ratios as those by aligned and 2D random models.

From the numerical results plotted in Figs. 2–7, it is shown that the M–T relations given in Eqs. (19) and (22) can be applied to all range of the filler aspect ratio ($0 < a < \infty$), and the filler

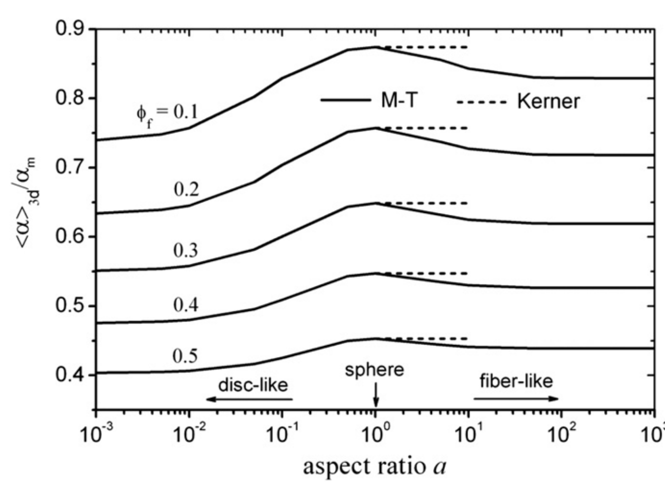

Fig. 7. Variation of coefficients of thermal expansion with aspect ratio a by 3D random M–T and Kerner results.

orientation effects can also be accounted properly. Compared to other models discussed, M–T model is suitable for more general problems of composites with different filler shapes. The explicit expressions of M–T model for several specific cases, such as sphere ($a = 1$), disc-like ($a \to 0$) and cylinder-like ($a \to \infty$) fillers, have been obtained in earlier literature [14]. The general expressions with the parameter of filler aspect ratio in Eqs. (22) and (19) are amended ones obtained by Chow [2,3] and by Lee et al. [1], respectively, and have been proved to be identical in this work. This verification is useful to avoid misusing M–T relations in future applications.

In some of theories in literature on predicting mechanical and thermal properties of composites using M–T models, the local coordinate systems established for the fiber-like and the disk-like spheroidal inclusions, respectively, were set to be different, i.e. x_1 being defined to be the axis of rotation symmetry for the fiber-like spheroidal inclusions while x_3 being defined to be the axis of rotation symmetry for the disk-like ones (see, for examples [1,29],). For identification, the notations // and $\perp$ were further introduced to indicate directions parallel and perpendicular to the axis of rotation symmetry for both fiber-like and disk-like spheroidal inclusions [24]. As discussed in the subsection 3.3, the components of Eshelby tensor are directly related to the coordinate system defined for the spheroidal inclusions. Therefore, care should be taken when using Eqs. (19) and (22) for predicting the CTEs of composites with disk-like fillers in this case because as mentioned above the relations given in Eqs. (19) and (22) together with the components of Eshelby tensor given in Appendix 2 are all expressed based on the coordinate system for spheroidal inclusion defined in Fig. 1, i.e. x_1 being defined to be the axis of spheroid rotation symmetry. Proper cyclic permutations of (1,2,3) for the components S_{ijkl} of Eshelby tensor, as done in the subsection 3.3, may be required in this case.

For not causing possible confusing in practical applications, both fiber-like and disk-like spheroidal inclusions ($a_1 \neq a_2 = a_3$) can be defined uniformly in the same coordinate system, as treated in this paper, and are distinguished by the aspect ratio $a = a_1/a_3$ only, i.e. $a > 1$ for fiber-like fillers and $a < 1$ for disk-like fillers. Since $a_2 = a_3$ for the spheroidal inclusions, the composites with both fiber- and disk-like shaped fillers show transversely isotropic properties in x_2x_3 plane. Therefore, for the CTEs of composites with both fiber- and disk-like aligned fillers predicted by Eqs. (19) and (22), one always has

$$\alpha_{\|} = \alpha_{11}, \quad \alpha_{\perp} = \alpha_{22} = \alpha_{33} \tag{30}$$

Under the unified coordinate system, variations of CTEs with respect to filler aspect ratios can be plotted naturally in whole range $0 < a < \infty$ as shown in Figs. 4, 5 and 7, and thermal expansion properties of composites with both fiber-like and disk-like fillers can be compared and discussed distinctly with the graphs.

5. Concluding remarks

By comparing the expressions of CTEs for aligned composites obtained in Eq. (19) with those given in Refs. [3] and [1], it is found that there existed certain small errors overlooked in both of their relations. By eliminating the flaws, the calculated results by all the relations are proved to be exactly same. This indicates that although with somewhat different treatments in derivations the models presented by both Chow [3] and Lee et al. [1] are essentially belong to the framework of M–T model, and offer identical predicting results. This verifies the correctness of the consistency property of M–T models discussed in Ref. [6] and clarifies the points raised in introduction.

As mentioned in the preceding sections, some relations of M–T models for CTEs available in literature, such as the relations by Chow [3] and Lee et al. [1], may be obtained under different coordinate systems established for spheroidal inclusions. Since element arrangements of Eshelby tensor are coordinate system related, the components of Eshelby tensor with same subscript number under different coordinate systems defined may have different expressions. Therefore, special attention should be taken to use correct expressions of Eshelby tensor components in applying different relations of M–T models for predictions. It is likely to be overlooked in practical applications, which may lead to incorrect predictions.

In various theory models on CTEs available in literature, M–T models offer direct predictions based on the information of mechanical and thermal properties of matrix and fillers only and can effectively account for the effects of fillers' aspect ratios from disc-like to fiber-like ranges and orientation, as discussed in the numerical studies. These distinct characters have made M–T models very suitable for predicting mechanical and thermal properties of nanocomposites in applications. For convenience of using different relations of M–T models, the original relations of Chow [3] have been converted to be expressed in the forms consistent with the coordinate system defined for spheroidal inclusions shown in Fig. 1 and the components of Eshelby tensor given in Appendix 2. The self-consistent relations of M–T models for CTEs presented and related issues discussed in this work may be helpful for proper use of M–T models in applications.

Acknowledgment

This paper is dedicated to the author's father, Lu Jishan (吕继山).

Appendix 1

Consider a composite with finite volume fractions of matrix and N different types of fillers defined by ϕ_m and ϕ_{f_i} ($i = 1,2,\ldots,N$), respectively, in which ϕ_{f_i} is the volume fraction of the ith filler. The volume fractions satisfy the relation $\phi_m = \sum_{i=1}^{N} \phi_{f_i} = 1$. The elastic moduli tensors for the matrix and the filler phases are denoted by C^m and C_i^f ($i = 1,2,\ldots,N$), respectively, and the thermal expansion coefficients of the matrix and the fillers are denoted by α^m and α^{f_i} ($i = 1,2,\ldots,N$), respectively. When the composite is subjected to a uniform temperature change ΔT, the misfit strain caused by the difference of the thermal expansion coefficients between the matrix and the ith filler is given by

$$\varepsilon_{f_i}^{\Delta T} = \left(\alpha^{f_i} - \alpha^m\right)\Delta T \tag{A1.1}$$

With the uniform temperature change, the thermal expansion in the homogeneous matrix without any inclusion is uniform and the elastic field in the matrix is not generated. However, a certain average perturbed strain $\tilde{\varepsilon}^m$ has been introduced due to the presence of inclusions. This perturbed strain corresponds to an average perturbed stress $\tilde{\sigma}^m$ through the elastic constants C^m of the matrix. Thus, the constitutive relation in the matrix after the perturbation is

$$\tilde{\sigma}^m = C^m \tilde{\varepsilon}^m \tag{A1.2}$$

Furthermore, define $\tilde{\sigma}^{f_i}$ and $\tilde{\varepsilon}^{f_i}$ to be the average perturbed stress and strain in the ith particle with respect to the matrix. According to Eshelby equivalent principle, the average stress in the particles may be written as

$$\tilde{\sigma}^m = \tilde{\sigma}^{f_i} = C^{f_i}\left(\tilde{\varepsilon}^m + \tilde{\varepsilon}^{f_i} - \varepsilon_{f_i}^{\Delta T}\right) = C^m\left(\tilde{\varepsilon}^m + \tilde{\varepsilon}^{f_i} - \varepsilon_{f_i}^{\Delta T} - \varepsilon_{f_i}^{*}\right), \ (i = 1,2,\ldots,N) \tag{A1.3}$$

where $\varepsilon^*_{f_i}$ is the average equivalent transformation strains of the particle. Accoding to Eshelby's solutions for the inhomogeneity with its own eigenstrains [27], we have

$$\tilde{\varepsilon}^{f_i} = S^{f_i}\left(\varepsilon^{\Delta T}_{f_i} + \varepsilon^*_{f_i}\right), \quad (i = 1, 2, \ldots, N) \tag{A1.4}$$

where S^{f_i} is Eshelby's tensors for the domain of the ith filler.

Since the composite is not subjected any external traction, the average of the stresses over the matrix and particles should be zero, i.e. $\tilde{\sigma}^m + \sum_{i=1}^N \phi_{f_i}\tilde{\sigma}^{f_i} = 0$. From Eqs. (A1.2) and (A1.3), and making use of the relation (A1.4), this gives

$$\tilde{\varepsilon}^m = -\sum_{i=1}^N \phi_{f_i}\left(\tilde{\varepsilon}^{f_i} - \varepsilon^{\Delta T}_{f_i} - \varepsilon^*_{f_i}\right) = -\sum_{i=1}^N \phi_{f_i}\left(S^{f_i} - I\right)\left(\varepsilon^{\Delta T}_{f_i} + \varepsilon^*_{f_i}\right) \tag{A1.5}$$

substituting Eqs. (A1.4) and (A1.5) into (A1.3) yields

$$\left\{\left(C^{f_i} - C^m\right)\left[S^{f_i} - \sum_{i=1}^N \phi_{f_i}\left(S^{f_i} - 1\right)\right] + C^m\right\}\left(\varepsilon^{\Delta T}_{f_i} + \varepsilon^*_{f_i}\right) = C^{f_i}\varepsilon^{\Delta T}_{f_i} \tag{A1.6}$$

from which $\varepsilon^{\Delta T}_{f_i} + \varepsilon^*_{f_i}$ can be solved in term of $\varepsilon^{\Delta T}_{f_i}$ as

$$\varepsilon^{\Delta T}_{f_i} + \varepsilon^*_{f_i} = \left\{\left(C^{f_i} - C^m\right)\left[S^{f_i} - \sum_{i=1}^N \phi_{f_i}\left(S^{f_i} - 1\right)\right] + C^m\right\}^{-1} C^{f_i}\varepsilon^{\Delta T}_{f_i} \tag{A1.7}$$

On the other hand, the volume average strain of the composite caused by $\varepsilon^{\Delta T}_{f_i}$ $(i = 1,2,\ldots,N)$ is given by $\overline{\varepsilon} = \phi_m\tilde{\varepsilon}^m + \sum_{i=1}^N \phi_{f_i}(\tilde{\varepsilon}^m + \tilde{\varepsilon}^{f_i})$. From Eqs. (A1.4) and (A1.5), this gives [27]

$$\overline{\varepsilon} = \sum_{i=1}^N \phi_{f_i}\left(\varepsilon^{\Delta T}_{f_i} + \varepsilon^*_{f_i}\right) \tag{A1.8}$$

Therefore, the total average strain over the whole composite under the uniform temperature change is the sum of the thermal strain, $\alpha^m\Delta T$, generated by the temperature change and the average strain $\overline{\varepsilon}$ due to the total eigenstrain in the equivalent particles. According to the definition of thermal expansion coefficient, the total average strain in the composite by ΔT can be expressed as $\overline{\alpha}\Delta T$. The effective thermal expansion coefficient of the composite, $\overline{\alpha}$, thus is given by

$$\overline{\alpha} = \alpha^m + \sum_{i=1}^N \phi_{f_i}\left(\varepsilon^{\Delta T}_{f_i} + \varepsilon^*_{f_i}\right)\Big/\Delta T \tag{A1.9}$$

By substituting Eqs. (A1.8) and (A1.1) into Eq. (A1.9), we obtain the effective thermal expansion coefficient as

$$\overline{\alpha} = \alpha^m + \sum_{i=1}^N \phi_{f_i}\left\{\left(C^{f_i} - C^m\right)\left[S^{f_i} - \sum_{i=1}^N \phi_{f_i}\left(S^{f_i} - I\right)\right] + C^m\right\}^{-1} \times C^{f_i}\left(\alpha^{f_i} - \alpha^m\right) \tag{A1.10}$$

Appendix 2. Eshelby tensors

For a spheroidal inclusion with the axis of rotation symmetry identified as x'_1 $x'_1 (a_1 \neq a_2 = a_3)$ as shown in Fig. 1, the components of Eshelbys tensor for the spheroidal inclusion are

$$\begin{aligned}
S_{1111} &= \frac{1}{2(1-\nu_m)}\left\{1 - 2\nu_m + \frac{3a^2-1}{a^2-1} - \left[1 - 2\nu_m + \frac{3a^2}{a^2-1}\right]g\right\} \\
S_{2222} = S_{3333} &= \frac{3}{8(1-\nu_m)}\frac{a^2}{a^2-1} + \frac{1}{4(1-\nu_m)}\left[1 - 2\nu_m - \frac{9}{4(a^2-1)}\right]g \\
S_{2233} = S_{3322} &= \frac{1}{4(1-\nu_m)}\left\{\frac{a^2}{2(a^2-1)} - \left[1 - 2\nu_m + \frac{3}{4(a^2-1)}\right]g\right\} \\
S_{2211} = S_{3311} &= -\frac{1}{2(1-\nu_m)}\frac{a^2}{a^2-1} + \frac{1}{4(1-\nu_m)}\left[\frac{3a^2}{a^2-1} - (1-2\nu_m)\right]g \\
S_{1122} = S_{1133} &= -\frac{1}{2(1-\nu_m)}\left[1 - 2\nu_m + \frac{1}{a^2-1}\right] \\
&\quad + \frac{1}{2(1-\nu_m)}\left[1 - 2\nu_m + \frac{3}{2(a^2-1)}\right]g \\
S_{2323} = S_{3232} &= \frac{1}{4(1-\nu_m)}\left\{\frac{a^2}{2(a^2-1)} + \left[1 - 2\nu_m - \frac{3}{4(a^2-1)}\right]g\right\} \\
S_{1212} = S_{1313} &= \frac{1}{4(1-\nu_m)}\left\{1 - 2\nu_m - \frac{a^2+1}{a^2-1} - \frac{1}{2}\left[1 - 2\nu_m - \frac{3(a^2+1)}{a^2-1}\right]g\right\}
\end{aligned} \tag{A2.1}$$

where ν_m is the Poisson ratio of the matrix, a is the aspect ratio of the inclusion ($a = a_1/a_3$), and g is given by

$$g = \begin{cases} \dfrac{a}{\left(a^2-1\right)^{3/2}}\left\{a\left(a^2-1\right)^{1/2} - \cosh^{-1}a\right\}, & \text{prolate shape}(a_1 > a_2 = a_3) \\ \dfrac{a}{\left(1-a^2\right)^{3/2}}\left\{\cos^{-1}a - a\left(1-a^2\right)^{1/2}\right\}, & \text{oblate shape } (a_1 < a_2 = a_3) \end{cases} \tag{A2.2}$$

For a spherical inclusion with $a_1 = a_2 = a_3$, the components of the Eshelby matrix are simplified to

$$\begin{aligned} S_{1111} &= S_{2222} = S_{3333} = \frac{7-5\nu_m}{15(1-\nu_m)} \\ S_{1122} &= S_{2233} = S_{3311} = \frac{5\nu_m-1}{15(1-\nu_m)} \\ S_{1212} &= S_{2323} = S_{3131} = \frac{4-5\nu_m}{15(1-\nu_m)} \end{aligned} \tag{A2.3}$$

For a needle or circular cylinder with $a = a_1/a_3 \to \infty$, we have

$$\begin{aligned} & S_{1111} = 0,\ S_{1122} = S_{1133} = 0,\ S_{2222} = S_{3333} = \frac{5-4\nu_m}{8(1-\nu_m)} \\ & S_{2233} = S_{3322} = \frac{4\nu_m-1}{8(1-\nu_m)},\ S_{2211} = S_{3311} = \frac{\nu_m}{2(1-\nu_m)} \\ & S_{2323} = \frac{3-4\nu_m}{8(1-\nu_m)},\ S_{1212} = S_{1313} = \frac{1}{4} \end{aligned} \tag{A2.4}$$

For a penny-shaped disc with an aspect ratio $a = a_1/a_3 \ll 0$, they are

$$\begin{aligned} & S_{1111} = 1 - \frac{1-2\nu_m}{4(1-\nu_m)}\pi a,\ S_{2222} = S_{3333} = -\frac{13-8\nu_m}{32(1-\nu_m)}\pi a \\ & S_{2233} = S_{3322} = \frac{8\nu_m-1}{32(1-\nu_m)}\pi a,\ S_{2211} = S_{3311} = \frac{2\nu_m-1}{8(1-\nu_m)}\pi a \\ & S_{1122} = S_{1133} = \frac{\nu_m}{1-\nu_m}\left[1 - \frac{1+4\nu_m}{8\nu_m}\pi a\right] \\ & S_{2323} = \frac{7-8\nu_m}{32(1-\nu_m)}\pi a,\ S_{1212} = S_{1313} = \frac{1}{2}\left[1 - \frac{2-\nu_m}{4(1-\nu_m)}\pi a\right] \end{aligned} \tag{A2.5}$$

For a thin disc with $a = a_1/a_3 \to 0$, the only nonvanishing components are

$$S_{1111} = 1, \quad S_{1122} = S_{1133} = \frac{\nu_m}{1-\nu_m}, \quad S_{1212} = S_{1313} = \frac{1}{2} \tag{A2.6}$$

References

[1] Lee KY, Kim KH, Jeoung SK, Ju SI, Shim JH, Kim NH, et al. Polymer 2007;48:4174–83.
[2] Chow TS. J Polym Sci Polym Phys Ed 1978;16:959–65.
[3] Chow TS. J Polym Sci Polym Phys Ed 1978;16:967–70.
[4] Eshelby JD. Proc R Soc London 1957;A241:376–96.
[5] Mori T, Tanaka K. Acta Metall 1973;21:571–4.
[6] Benveniste Y, Dvorak GJ. On a correspondence between mechanical and thermal effects in two-phase composites. In: Weng GJ, Taya M, Abe H, (Eds), Micromechanics and inhomogeneity. New York: Springer-Verlag; 1990. p. 65–81.
[7] Turner PS. J Res Natl Bur Stand 1946;37:239–60.
[8] Kerner EH. Proc Phys Soc B 1956;69:808–13.
[9] Levin VM. Mekhanika Tverdogo Tela 1967;2:88–94.
[10] Schapery RA. J Compos Mater 1968;2:380–404.
[11] Rosen BW, Hashin Z. Int J Eng Sci 1970;8:157–73.
[12] Hsieh CL, Tuan WH. Mater Sci Eng A 2007;460-461:453–8.
[13] Milhans J, Ahzi S, Garmestani H, Khaleel MA, Sun X, Koeppel BJ. Mater Des 2009;30:1667–73.
[14] Wakashima K, Otsuka M, Umekawa S. J Compos Mater 1974;8:391–404.
[15] Takahashi K, Harakawa K. J Compos Mater 1980;14:144–59.
[16] Chou TW, Nomura S. Fibre Sci Tech 1980–81;14:279–91.
[17] Takao Y, Taya M. J Appl Mech 1985;52:806–10.
[18] Arsenault RJ, Taya M. Acta Metall 1987;35:651–9.
[19] Takei T, Hatta H, Taya M. Mater Sci Eng A 1991;131:133–43.
[20] Tane M, Hyun SK, Nakajima H. Scrip Mater 2006;54:545–52.
[21] Lee KY, Hong SR, Jeoung SK, Ju SI, Kim NH, Lee SG, et al. Polymer 2008;49:2146–52.
[22] Yoon PJ, Fornes TD, Paul DR. Polymer 2002;43:6727–41.
[23] Kim H, Macosko CW. Polymer 2009;50:3797–809.
[24] Spencer MW, Paul DR. Polymer 2011;52:4910–9.
[25] Cho M, Jang J, Suhr J. J Nanosci Nanotechno 2011;11:1098–102.
[26] Benveniste Y. Mech Mater 1987;6:147–57.
[27] Mura T. Micromechanics of defects in solids. 2nd ed. Dordrecht: Martinus Nijhoff Publishers; 1987 [Chapters 2, 4 and 7].
[28] Tandon GP, Weng GJ. Polym Compos 1984;5:327–33.
[29] Lee KY, Paul DR. Polymer 2005;46:9064–80.